Densification and deformation studies on powder metallurgy Al–TiO_2–Gr composite during cold upsetting

Manickam Ravichandran and Abdullah Naveen Sait[a)]
Department of Mechanical Engineering, Chendhuran College of Engineering and Technology, Pudukkottai 622 507, Tamilnadu, India

Veeramani Anandakrishnan
Department of Production Engineering, National Institute of Technology, Tiruchirappalli 620 015, Tamilnadu, India

(Received 30 April 2014; accepted 17 June 2014)

Aluminum metal matrix hybrid composites were synthesized through powder metallurgy route from ball milled powders to yield the compositions: Al + 0% TiO_2, Al + 2.5% TiO_2, Al + 2.5% TiO_2 + 2% Gr, and Al + 2.5% TiO_2 + 4% Gr. The densification and deformation properties of sintered Al–TiO_2–Gr composites during cold upsetting were investigated experimentally. The powder preforms are compacted using suitable punch and die in 40 kN hydraulic press and the initial percentage theoretical density was maintained as 85%. Sintering was done in an electric muffle furnace at the temperature of 590 °C for a period of 3 h. The sintered preforms were subjected to incremental compressive loading of 10 kN until cracks were found at the free surface. The true axial stress (σ_z), true hoop stress (σ_θ), true hydrostatic stress (σ_m), and true effective stress (σ_{eff}) were calculated for all the preforms and all these stresses are correlated with the true axial strain (ε_z). The densification behaviors of the composites were studied against true axial strain (ε_z) and lateral strain. Better densification and deformation property were obtained for pure aluminum preforms compared with other composite preforms. Addition of TiO_2 to the pure Al and Gr reinforcements increases the strength coefficient of the Al–TiO_2 composite.

I. INTRODUCTION

Metal matrix composites (MMCs) are a relatively new class of materials characterized by lighter weight and greater strength than those of conventional materials. MMCs are under attention for many applications in aerospace, defense, and automotive industries. Among the all MMCs, aluminum metal matrix composites (AMMCs) are being considered as a group of new advanced materials for its light weight, high strength, low thermal expansion coefficient, and good wear resistance. AMMCs have been prepared for various applications in aerospace, automotive, military, and electronic industry due to their excellent properties.[1] In MMCs, the reinforcements are added to the matrix material to improve the mechanical properties of composites. On the other hand, the use of single reinforcement in an aluminum (Al) matrix may sometimes affect the other mechanical as well as physical properties of the composite. To overcome this difficulty, two reinforcements are added to the matrix material to produce the hybrid composites. Ravindran et al. fabricated Al–SiC–Gr hybrid powder metallurgy (PM) composite and reported that the addition of both hard reinforcement like SiC and soft reinforcement like graphite improves the wear resistance of Al composites significantly.[2] Ted Guo and Tsao studied the tribological behavior of self-lubricating Al–SiC–graphite hybrid composites synthesized by the semisolid powder-densification method and reported that the strength is increased by the SiC and the lubrication property is enhanced by the graphite.[3] Mahdavi and Akhlaghi analyzed the effect of graphite content on the tribological behavior of Al/Gr and Al/30SiC/Gr composites processed by in situ PM method and concluded that the addition of graphite to the Al matrix composite reduces the porosity and also the wear rate.[4] Several groups of both hard and soft reinforcements were used for the fabrication of AMMCs through various manufacturing routes. Along with all the reinforcements, titanium dioxide (TiO_2) also introduced as a new type of hard reinforcement because of its very good mechanical property, corrosion resistance, and wear resistance.[5] Additionally, TiO_2 is one of the most extensively used oxides because of its remarkable optical and electrical properties.[6] Among the various composite manufacturing technologies, PM is the most unique manufacturing approach. The advantage of PM is the ability to fabricate high class, complex parts to close tolerances in an inexpensive manner. In PM, the solid metallic materials and components are produced from metallic powders.

[a)]Address all correspondence to this author.
e-mail: naveensait@yahoo.co.in
DOI: 10.1557/jmr.2014.143

 © Materials Research Society 2014

https://doi.org/10.1557/jmr.2014.143 Published online by Cambridge University Press

The fundamental manufacturing steps in PM include mixing of powders, compacting, and sintering. The microstructure of the PM materials is as similar as cast and wrought parts but pore related microstructural parameters can be taken into account for the study of mechanical and tribological properties.[7] Narayanasamy et al. investigated on the cold forging of sintered aluminum–3.5% alumina PM composite under triaxial stress state condition and also suggested that the cold deformation study on the sintered PM composites is very important for the fabrication of PM parts in various applications.[8] They also studied about the effect of particle size on Al–iron PM composite during cold upsetting. Also the density coefficient, strain hardening exponent, strain rate sensitivity, and strength coefficient with respect to increasing the relative density were discussed for the different percentages of iron.[9] Narayanasamy et al. investigated the effect of geometric work-hardening and matrix work-hardening on workability and densification of Al–3.5% alumina composite during cold upsetting and explained about the importance of densification and deformation studies on PM porous material.[10]

Although a large volume of the literature is available on the synthesis of PM – Al composites using other reinforcements, very little attention has been given to the TiO_2 reinforced composites. Therefore, in this study, the densification and deformation behavior of Al–TiO_2–Gr hybrid composites have been studied. The XRD analysis of the powder blends was carried out to study the formation of composites and SEM analysis was carried out to reveal the surface morphological features of the ball milled powders and sintered composites. The strength coefficient, strain coefficient and various stresses like true axial stress (σ_z), true hoop stress (σ_θ), true hydrostatic stress (σ_m), and true effective stress (σ_{eff}) induced during the cold upsetting have also been studied.

II. EXPERIMENTAL DETAILS

Atomized Al powder of 99.7% purity supplied by Kemphasol (Mumbai, India) was used as the matrix material and rutile phase of TiO_2 and Gr powders supplied by Acechemie (India) is used as the reinforcement material. The chemical composition of as-received PM aluminum has been given in Table I. The reinforcement materials (TiO_2 and Gr) are blended with Al in the weight percentages to yield the different composites namely, Al + 0% TiO_2, Al + 2.5% TiO_2, Al + 2.5% TiO_2 + 2% Gr, and Al + 2.5% TiO_2 + 4% Gr for the present work.

TABLE I. Chemical composition of as-received aluminum powder.

Fe	Mn	Ti	N	Si	Cu	Al
0.1	0.2	0.03	0.006	0.1	0.02	99.7

The required mass of Al, TiO_2, and Gr was accurately weighed in an electronic weighing machine and blended in ball mill for 12 h. The balls and powders weight ratio was 1:1 and the speed (rpm) of the drum was calculated by the formula $N = 32/\sqrt{D}$,[11] where D is the diameter of the drum. The powder mixtures were compacted into cylindrical billets of diameter 24 mm and height 12 mm using computerized universal testing machine of 400 kN capacity, to obtain the green compacts at 85% theoretical density. Graphite mixed with lubricant oil was used as the lubricant during compaction. An indigenously developed ceramic coating was applied on the free surfaces of the compacts and dried under room temperature for a period of 12 h. The ceramic coated compacts were sintered in an electric muffle furnace in the temperature range of 590 ± 10 °C for a period of 3 h and cooled to room temperature in the furnace itself. The sintered green compacts were cleaned and measurements such as initial height (H_0), diameter (D_0), and mass (m) were carried out to find the strain and initial density. The cold upsetting being carried out between two flat high speed steel dies. During the cold upsetting test, graphite lubricant was used at both the die contact surfaces, to ensure the minimum friction, resulting in homogenous deformation. The incremental compressive load is applied on the cold upset specimen, until fine cracks appeared on its free surface. After each interval of loading dimensional changes in the specimen such as height after deformation (H_d), top contact diameter (D_{TC}), bottom contact diameter (D_{BC}), bulged diameter (D_B), and final density of the preform (ρ_f) were measured. Archimedes principle was used to find the actual densities of the preforms. The measured values were used to calculate the true axial stress (σ_z), true hoop stress (σ_θ), true hydrostatic stress (σ_m), true effective stress (σ_{eff}), true axial strain (ε_z), lateral strain, percentage theoretical density (%ρ_{th}), and *Poisson's* ratio (α) which provided the basis for the densification and deformation studies of the hybrid composites.

The true hoop stress (σ_θ) of the Al–TiO_2–Gr composite was calculated using the below given expression,[10]

$$\sigma_\theta = \frac{(1+2\alpha)}{2+\alpha}\sigma_z \quad , \tag{1}$$

where α is Poisson's ratio and σ_z is true axial stress.

The true hydrostatic stress (σ_m) of the Al–TiO_2–Gr composite was calculated by using the below given expressions suggested by Narayanasamy et al.[12]

$$\sigma_m = \frac{(\sigma_\theta + \sigma_z)}{3} \quad . \tag{2}$$

The true effective stress (σ_{eff}) can be calculated by using the below given expression,[12]

https://doi.org/10.1557/jmr.2014.143 Published online by Cambridge University Press

$$\sigma_{eff} = (0.5 + \alpha)[3(1 + \alpha + \alpha^2)]^{0.5}\sigma_z \quad . \qquad (3)$$

III. RESULTS AND DISCUSSION

A. XRD analysis for composite powders

Figure 1 shows the XRD patterns of the Al + 0% TiO_2, Al + 2.5% TiO_2, Al + 2.5% TiO_2 + 2% Gr, and Al + 2.5% TiO_2 + 4% Gr composite powders ball milled for 12 h. PANalytical X'Pert x-ray diffractometer (PANalytical, EA Almalo, Netherlands) Cu K_α target (λ = 1.5418 Å) was used to carry out the XRD analysis of powder blends. The crystallinity of the pure Al was clearly evident (Fig. 1) by the sharper diffraction peaks at the respective diffraction angles which can be readily indexed for its cubic structure and it is compatible with the standard JCPDS data (Card No. 85-1327). From Fig. 1, the XRD analysis reveals the presence of Al, TiO_2, and Gr phases. However, it shows a modification of the intensity and the shape of peaks when the powder was mechanically activated. These modifications can be due to a size decrease and an increase of the residual lattice distortions. Moreover, a slight shift of the XRD profile after ball milling was observed. This decrease of the lattice parameter can be due to TiO_2 and Gr substituting Al in the network.

B. SEM analysis for composite powders

SEM images of the as-produced mixture of Al, TiO_2, and Gr powder particles in various weight percentages are shown in Figs. 2(a)–2(d). The morphology of the as-received Al powder particles is shown in Fig. 2(a) and the shape of the particles appeared as ligament. Figure 2(b) shows the uniform distribution of TiO_2 powder particles on the Al matrix. It can be seen that the TiO_2 particles distributed evenly within the Al powder particles and there is no agglomeration of TiO_2 with Al particles in the mixture produced by the PM ball milling process. From Figures 2(c) and 2(d), the uniform distribution of Gr with the Al + 2.5% TiO_2 composite blends and also the cold welding mechanism of the matrix and reinforcement material (TiO_2 and Gr) during the mechanical ball milling can be observed. The hard reinforced particles are cold welded with the soft Al matrix. After ball milling, the shape of the particles is changed and it seems to be round and ligament.

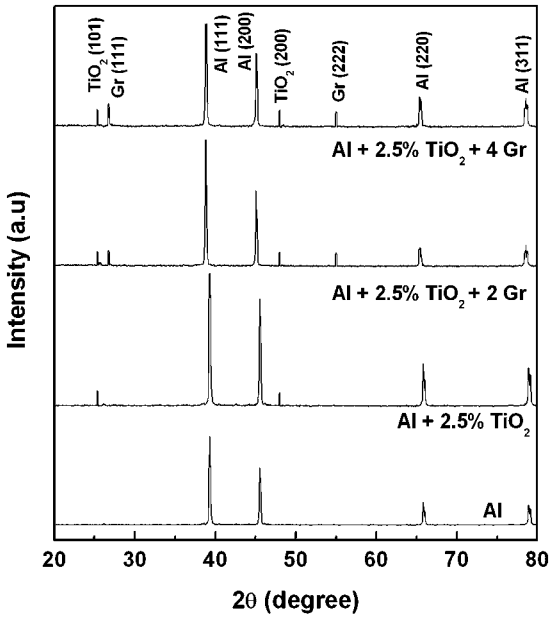


FIG. 1. XRD patterns of as-received aluminum powder and as-produced mixture of aluminum and various weight percentages of TiO_2 and graphite powder particles.

C. Stress analysis

The analysis of true stress and true strain is very important to study the deformation characteristics of a material during any cold working operation.[13] In the present work, various stresses like true axial stress (σ_z), true hoop stress (σ_θ), true hydrostatic stress (σ_m), and true effective stress (σ_{eff}) induced during the cold upsetting have also been studied. The densification and deformation studies of the preforms were carried out by relating the percentage theoretical density with true axial strain (ε_z), lateral strain, and true axial stress (σ_z).

1. True axial stress (σ_z) versus true axial strain (ε_z)

The true axial stress (σ_z) during the cold upsetting of the PM sintered aluminum composites has been calculated from the values of axial applied load and contact area of the Al–TiO_2–Gr composite. The true axial strain (ε_z) was calculated from the deformed height and the undeformed height. All the measurements were taken accurately using a digital vernier. Figure 3 shows the plots of true axial stress (σ_z) versus true axial strain (ε_z) during cold upsetting. From the graph, it is clearly evident that the plain Al compacts have higher true axial strain (ε_z). It means that the plain Al preforms exhibit better deformation property for the lower true axial stress (σ_z). Addition of 2.5% TiO_2 to the Al matrix reduces the deformation and increases the true axial stress (σ_z) value. The presence of hard TiO_2 particles in the soft Al increases the strength and resists deformation. Addition of 2% of graphite particles to the Al + 2.5% TiO_2 composite shows an increase in true strain rate continuously increases with deformation for the higher true axial stress (σ_z). However, the presence of 4% of graphite increases the true axial stress (σ_z) but not much improvement in strain. From the graph, it has been concluded that the addition of TiO_2 and graphite particles increases the true axial strength of the composites.

https://doi.org/10.1557/jmr.2014.143 Published online by Cambridge University Press

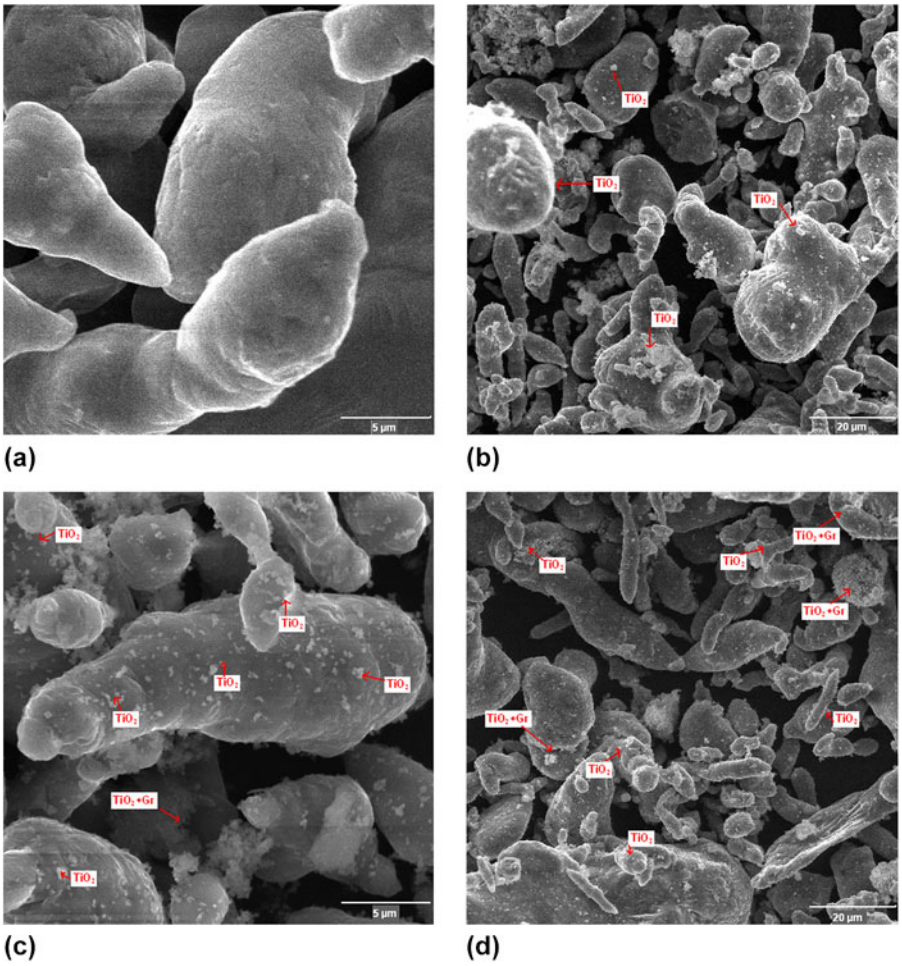


FIG. 2. SEM images of (a) as-received aluminum powders and (b–d) as-produced mixture of Al + 2.5% TiO_2, Al + 2.5% TiO_2 + 2% Gr, and Al + 2.5% TiO_2 + 4% Gr composite powders.

The true stress–strain curve is always called as flow curves. These curves are used to calculate the stress required to cause metal to flow plastically to any given strain. The relationship of true axial stress (σ_z) to true axial strain (ε_z) is no longer linear beyond the elastic region and perfectly fit in a power law curve with R^2 value very close to 1. Here, the power expression equation was used to calculate the strength coefficient and strain hardening coefficient, $\sigma = K\varepsilon^n$, where σ, true stress; ε, true strain; n, strain hardening exponent; K, strength coefficient. Hence, strength coefficient (K) and the strain hardening exponent (n) are calculated from the graph plotted between the true axial stress (σ_z) and true axial strain (ε_z).

The strength coefficient (K) and strain coefficient (n) for all the cold upset preforms are given in Table II. It can be clearly understood that the addition of reinforcement to the plain aluminum increases the strength of the composite. The addition of 2.5% of TiO_2 to the matrix increases the strength coefficient and decreases the strain

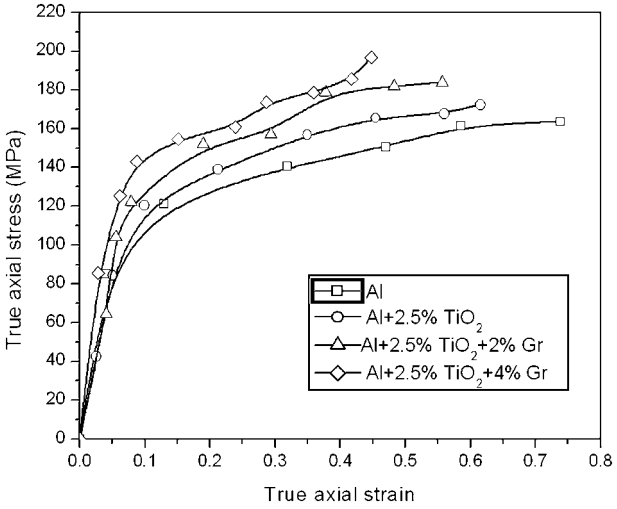


FIG. 3. True axial stress (σ_z) versus true axial strain (ε_z).

coefficient value because of its hard nature. However, the addition of 2% and 4% of graphite to the Al + 2.5% TiO_2 composite increases the strength coefficient as well as

https://doi.org/10.1557/jmr.2014.143 Published online by Cambridge University Press

strain coefficient values. The strength and strain of the Al + TiO_2 composite were highly influenced by the incorporation of graphite.

2. True axial stress versus lateral strain

Figure 4 shows the plots of true axial stress (σ_z) versus lateral strain during cold upsetting of Al + 0% TiO_2, Al + 2.5% TiO_2, Al + 2.5% TiO_2 + 2% Gr, and Al + 2.5% TiO_2 + 4% Gr composites. The lateral strain was calculated from the deformed and original diameter of the preforms. The true axial stress (σ_z) was correlated with lateral strain of the cold upset preforms. From Figs. 3 and 4, the axial and lateral deformation behavior of all the composites are similar. The highest lateral deformation was obtained for plain Al with lowest level of stress. Addition of reinforcements (TiO_2 and Gr) increases the strength and reduces the lateral deformation of the composites. The deformations are carried out in two stages. In the initial stage, the stress increases with a smaller increase in strain linearly. In the next stage, for a smaller increase in stress, the maximum strain was observed. Because of the addition of TiO_2 and Gr reinforcements, the Al–TiO_2–Gr composite requires a high level of stress for a smaller increase in strain.

TABLE II. Strength coefficient (K) and strain coefficient (n) values for each composition.

Sl. No.	Composites	Strength coefficient (K)	Strain coefficient (n)	R^2 value
1	Al + 0% TiO_2	175.5	0.210	0.974
2	Al + 2.5% TiO_2	189.6	0.189	0.991
3	Al + 2.5% TiO_2 + 2% Gr	214.7	0.216	0.984
4	Al + 2.5% TiO_2 + 4% Gr	246.0	0.274	0.940

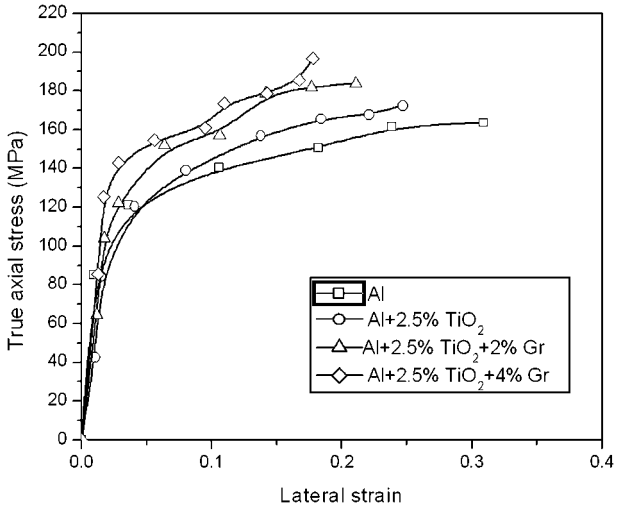


FIG. 4. True axial stress (σ_z) versus lateral strain (ε_z).

3. True hoop stress (σ_θ) versus and true axial strain (ε_z)

Fig. 5 shows the plot between the true hoop stress (σ_θ) and true axial strain (ε_z) of the PM preforms. The maximum hoop stress (189.17 MPa) was obtained for the Al + 2.5% TiO_2 + 4% Gr composite and the minimum hoop stress (σ_θ) (151.93 MPa) was found for the plain aluminum. The hoop stress (σ_θ) trend for Al + 2.5% TiO_2 composite was next to the plain aluminum. The increased hoop stress (σ_θ) was obtained for the composites containing Gr for the given true axial strain (ε_z).

4. True hydrostatic stress (σ_m) versus and true axial strain (ε_z)

Figure 6 has been plotted between true hydrostatic stress (σ_m) and true axial strain (ε_z) for the cold upset PM

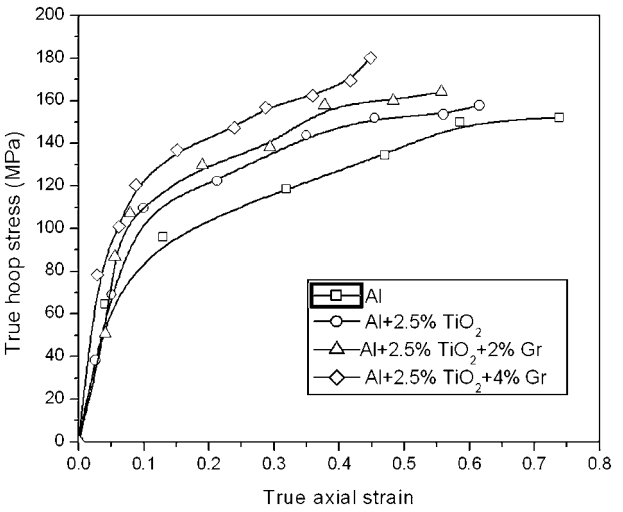


FIG. 5. True hoop stress (σ_θ) versus true axial strain (ε_z).

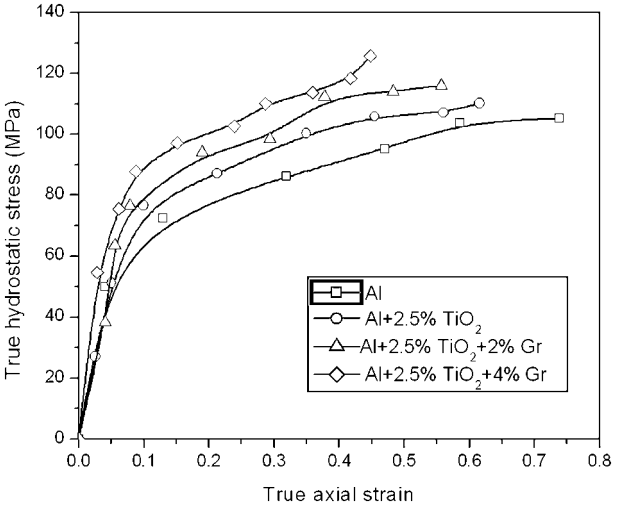


FIG. 6. True hydrostatic stress (σ_m) versus true axial strain (ε_z).

https://doi.org/10.1557/jmr.2014.143 Published online by Cambridge University Press

preforms. The triaxial compressive stress is called as hydrostatic pressure or hydrostatic stress (σ_m). This stress is resisting the fracture and increases the ductility during cold upsetting. The maximum hydrostatic stress (σ_m) was found for Al + 2.5% TiO_2 + 4% Gr composite and minimum for plain Al preforms. The trend of true hydrostatic stress (σ_m) versus true axial strain (ε_z) was observed as similar as true axial stress (σ_z) versus true height strain. The lowest true hydrostatic stress (σ_m) was obtained for the plain Al preforms. Without hydrostatic stress components, the plastic flow of materials cannot be achieved.[13] Here, 110.1037 MPa and 116.0631 MPa hydrostatic pressures are required for the Al + 2.5% TiO_2 and Al + 2.5% TiO_2 + 2% Gr composites to create the plastic flow during the cold upsetting.

5. True effective stress (σ_{eff}) versus and true axial strain (ε_z)

Figure 7 has been drawn between true effective stress (σ_{eff}) versus true axial strain (ε_z). The maximum true effective stress (σ_{eff}) (661.37 MPa) was obtained for the composites having 2.5% TiO_2 and 4% of graphite. The greatest deviation in true effective stress (σ_{eff}) was observed between the plain Al and composite compacts.

D. Densification studies

1. True axial stress versus percentage theoretical density

Figure 8 shows the graph drawn between the true axial stress (σ_z) and percentage theoretical density of composites during cold upsetting. Percentage theoretical density was calculated from the theoretical and actual density of the preforms. The actual density after each loading was found using Archimedes's principle to calculate the percentage theoretical density. During the compaction process, the initial green compact density was maintained as 85% of theoretical density. However, the density of the compacts increased during the sintering process because of bonding and welding mechanism of particles. From Fig. 8, it is clearly observed that the densification of the composites was carried out in two steps. In the initial stage, the densification is very low for the higher value of true axial stress (σ_z). In the second stage, the higher densification was achieved for lowest value of increase in stress. The maximum of 98% of theoretical density and the stress value of 164.4 MPa were observed for the plain Al preform. However, 98.36% densification was obtained for the Al + 2.5% TiO_2 + 2% Gr composite. But the applied stress for the hybrid composite was higher (184 MPa) than the plain Al preform. Composite contains 2% and 4% graphite having the similar trend of densification, but the required applied stress was higher than the composites without graphite. Poor densification was obtained for the Al + 2.5% TiO_2 composite and it can be understood that the addition of TiO_2 reinforcement decreases the densification. Addition of graphite to the Al + TiO_2 composite decreases the densification behavior of the hybrid composite (Fig. 8).

2. Percentage theoretical density versus true axial strain (ε_z)

The graph was drawn between the percentage theoretical density and true axial strain (ε_z) to study the densification and the axial deformation property of the composites during cold upsetting process. From Fig. 9, it is observed that the plain Al preforms have the better densification and deformation property. The addition of reinforcements like TiO_2 and graphite reduces the densification as well as deformation while comparing with plain Al preforms.

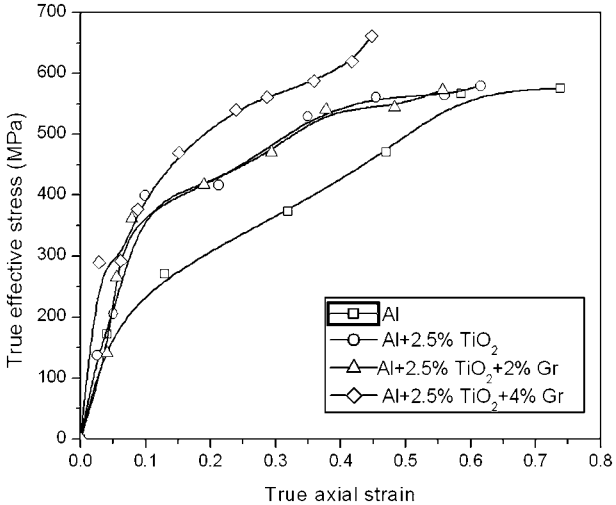


FIG. 7. True effective stress (σ_{eff}) versus true axial strain (ε_z).

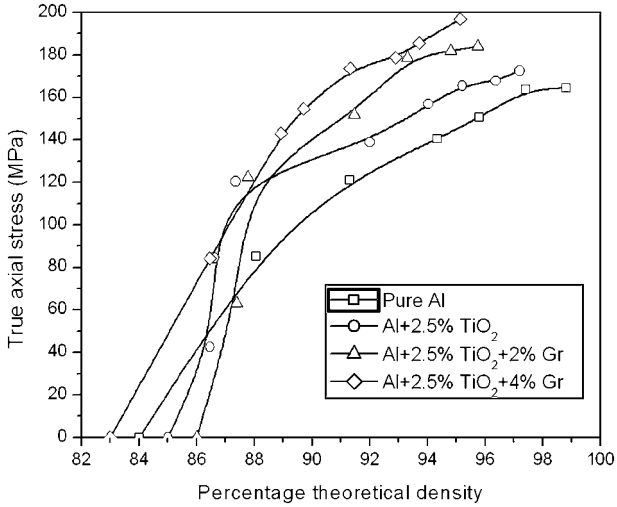


FIG. 8. True axial stress versus percentage theoretical density.

https://doi.org/10.1557/jmr.2014.143 Published online by Cambridge University Press

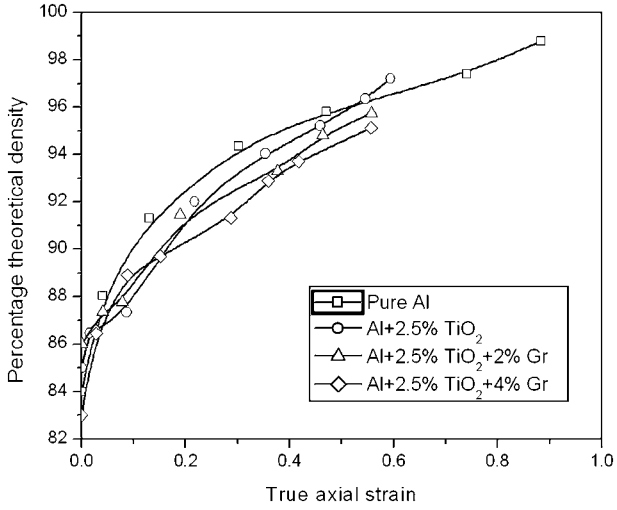


FIG. 9. Percentage theoretical density versus true axial strain.

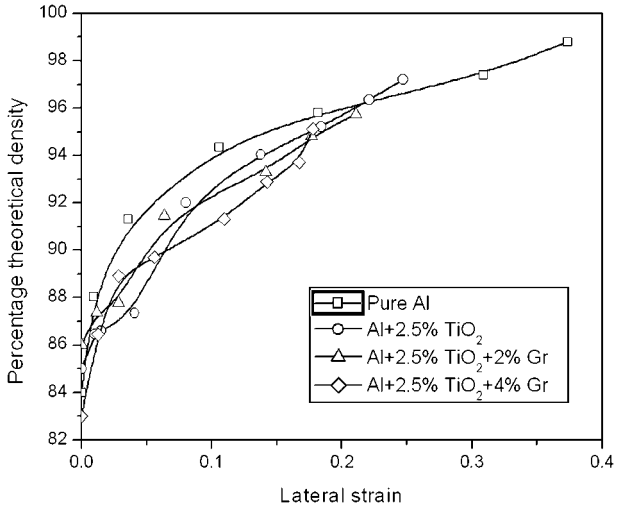


FIG. 10. Percentage theoretical density versus lateral strain.

Among the three composites tested, the Al + 2.5% TiO_2 + 2% Gr has the better densification and deformation property. The lowest value of densification and deformation was obtained for the Al + 2.5% TiO_2 + 4% Gr composite and it suggests that the addition of more weight percentage of reinforcement highly affects the densification and deformation property.

3. Percentage theoretical density versus true lateral strain

The graph between the percentage theoretical density and true lateral strain was drawn to study the densification and the lateral deformation property of the composites during cold upsetting of sintered PM preforms. Figures 9 and 10 clearly show that the axial and lateral deformation trends are very similar for all the preforms tested. Nevertheless, the rate of axial deformation was higher than the lateral deformation.

IV. CONCLUSION

AMMCs composed of TiO_2 and Gr as reinforcements were synthesized successfully by the PM method. The cold upset study has been carried out and the following conclusions are drawn

(1) The XRD patterns of the 12 h ball milled composite powders revealed the presence of matrix (Al) and reinforcements (TiO_2 and Gr) phases.

(2) SEM images that show the distribution of the reinforcement with the matrix material is homogenous and addition of reinforcements (TiO_2 and Gr) to the soft material influences the morphological characteristics of MMCs.

(3) High true axial stress (σ_z) and the maximum strength coefficient (K) were obtained for Al + 2.5% TiO_2 + 4% Gr hybrid composite and minimum for plain Al preform.

(4) Addition of 2.5% TiO_2 as the reinforcement to the Al matrix increases the strength and reduces the deformation of the composite.

(5) Better densification was obtained for the plain Al. The maximum of 98% of theoretical density was achieved for the plain Al preform. Addition of reinforcement to the plain Al reduces the densification property. The poor densification (94%) was obtained for the composites having 2.5% TiO_2 and 4% of Gr.

(6) Pure Al shows the better deformation and addition of TiO_2 to the matrix material highly influences the deformation property and also the strength of composites.

(7) The maximum true hoop stress (σ_θ), true effective stress (σ_{eff}), and hydrostatic static stress (σ_m) were attained for the Al + 2.5% TiO_2 + 4% Gr hybrid composite and minimum was obtained for plain Al preforms.

REFERENCES

1. M. Rahimian, N. Parvin, and N. Ehsani: The effect of production parameters on microstructure and wear resistance of powder metallurgy Al -Al_2O_3 composite. *Mater. Des.* **32**, 1031–1038 (2011).
2. P. Ravindran, K. Manisekar, P. Narayanasamy, N. Selvakumar, and R. Narayanasamy: Application of factorial techniques to study the wear of Al hybrid composites with graphite addition. *Mater. Des.* **39**, 42–54 (2012).
3. M.L. Ted Guo and C.Y.A. Tsao: Tribological behavior of self-lubricating aluminium/SiC/graphite hybrid composites synthesized by the semi-solid powder-densification method. *Compos. Sci. Technol.* **60**, 65–74 (2000).
4. S. Mahdavi and F. Akhlaghi: Effect of the graphite content on the tribological behavior of Al/Gr and Al/30SiC/Gr composites processed by in situ powder metallurgy (IPM) Method. *Tribol. Lett.* **44**, 1–12 (2011).
5. S. Sivasankaran, K. Sivaprasad, R. Narayanasamy, and V.K. Iyer: An investigation on flowability and compressibility of AA 6061_{100-x}-x wt.% TiO_2 micro and nanocomposite powder prepared by blending and mechanical alloying. *Powder Technol.* **201**, 70–82 (2010).

https://doi.org/10.1557/jmr.2014.143 Published online by Cambridge University Press

6. M.R. Vaezi: Two-step solochemical synthesis of ZnO/TiO_2 nanocomposite materials. *J. Mater. Process. Technol.* **205**, 332–337 (2008).
7. A. Mazahery and M.O. Shabani: Study on microstructure and abrasive wear behavior of sintered Al matrix composites. *Ceram. Int.* **38**, 4263–4269 (2012).
8. R. Narayanasamy, T. Ramesh, and K.S. Pandey: Some aspects on cold forging of aluminium-alumina powder metallurgy composite under triaxial stress state condition. *Mater. Des.* **29**, 1212–1227 (2008).
9. R. Narayanasamy, T. Ramesh, K.S. Pandey, and S.K. Pandey: Effect of particle size on new constitutive relationship of aluminium -iron powder metallurgy composite during cold upsetting. *Mater. Des.* **29**, 1011–1026 (2008).
10. R. Narayanasamy, V. Anandakrishnan, and K.S. Pandey: Effect of geometric work-hardening and matrix work-hardening on workability and densification of aluminium -3.5% alumina composite during cold upsetting. *Mater. Des.* **29**, 1582–1599 (2008).
11. R.M. German: *Powder Metallurgy Science*, 2nd ed. (Metal Powder Industries Federation, New Jersey, 1984).
12. K. Baskaran and R. Narayanasamy: An experimental investigation on work hardening behaviour of elliptical shaped billets of aluminium during cold upsetting. *Mater. Des.* **29**, 1240–1265 (2008).
13. G.E. Dieter: *Mechanical Metallurgy*, SI Metric ed. (McGraw-Hill Book Company, London, 1988).

https://doi.org/10.1557/jmr.2014.143 Published online by Cambridge University Press